

Time-dependent electron localization functions for coupled nuclear-electronic motion

M. Erdmann

Institut für Physikalische Chemie, Universität Würzburg, Am Hubland, 97074 Würzburg, Germany

E. K. U. Gross

Theoretische Physik, Freie Universität Berlin, Arnimallee 14, D-14195 Berlin, Germany

V. Engel^{a)}

Institut für Physikalische Chemie, Universität Würzburg, Am Hubland, 97074 Würzburg, Germany

(Received 26 July 2004; accepted 24 August 2004)

We study the quantum dynamics in a model system consisting of two electrons and a nucleus which move between two fixed ions in one dimension. The numerically determined wave functions allow for the calculation of time-dependent electron localization functions in the case of parallel spin and of the time-dependent antiparallel spin electron localization functions for antiparallel spin. With the help of these functions, it becomes possible to illustrate how electronic localization is modified through the vibrational wave-packet motion of the nucleus. © 2004 American Institute of Physics. [DOI: 10.1063/1.1806812]

In 1990, Becke and Edgecombe introduced a *simple measure of electron localization in atomic and molecular systems* in their such entitled article.¹ The authors defined the so-called electron localization function (ELF) within the Hartree-Fock theory and for systems with parallel spin. Up to now, many applications of the ELF to analyze atomic shell structure and bonding situations in molecules were presented, for a review see Ref. 2. Most recently, the ELF was employed in the time-domain to study the electronic dynamics of acetylene in a strong laser pulse and the collision of a proton with ethylene with *classically* moved nuclei.³ In this letter we elaborate on the idea of the ELF, extending the concept to a more general situation. In doing so, we exploit a model of two electrons and a nucleus all of which are allowed to move *quantum mechanically* in a single dimension between two ions, the latter being fixed in space. This particle configuration is sketched in Fig. 1.

We solve the time-dependent Schrödinger equation numerically exact to obtain wave functions $\psi(x\sigma, y\tau, R, t)$, where x, y, R are the electronic and nuclear coordinates, σ, τ are the spin coordinates of the electrons, and t denotes time. The wave functions serve as the starting point to calculate quantities which characterize electron localization. To proceed, we follow the strategy of Becke and Edgecombe, and start from the diagonal of the time-dependent density matrix of the two-electron/one-nucleus system, given by

$$D_{\sigma\tau}(x, y, R, t) = |\psi(x\sigma, y\tau, R, t)|^2. \quad (1)$$

This quantity is the probability density for finding, at time t , the two electrons with spins σ and τ at x and y , respectively, and the nucleus at position R . Although we might, in principle, investigate the localization of all three particles, we

concentrate here on the electrons. An average of the diagonal part of the density matrix over the nuclear degree of freedom yields

$$D_{\sigma\tau}(x, y, t) = \int dR D_{\sigma\tau}(x, y, R, t). \quad (2)$$

The time-dependent probability density (the electronic spin density) to find one electron with spin σ at point x , independently of where the other electron and the nucleus are located, is obtained by integration

$$\rho_{\sigma}(x, t) = \int d\tau \int dy D_{\sigma\tau}(x, y, t). \quad (3)$$

Furthermore we define the *conditional probability density* to find an electron with spin τ at y , if we know with certainty that another electron with spin σ is located at x , by

$$P_{\sigma\tau}(x, y, t) = \frac{D_{\sigma\tau}(x, y, t)}{\rho_{\sigma}(x, t)}. \quad (4)$$

We now have to distinguish the cases of parallel ($\alpha\alpha$) and antiparallel ($\alpha\beta$) spin of the two electrons. Since in the latter case, the coordinate-space wave function is symmetric with respect to exchange of the electrons, we may use the function

$$P_{\alpha\beta}(x, t) = P_{\alpha\beta}(x, x, t), \quad (5)$$

as a measure of localization. Accordingly, $P_{\alpha\beta}(x, t)dx$ is the conditional probability in the volume element dx to find one electron at time t at point x , if we know with certainty that the other electron with opposite spin is at the same place. Unfortunately, this relation is an indirect one. $P_{\alpha\beta}(x, t)$ is small, if the electron at x is strongly localized. Following the example given by Becke and Edgecombe for the ELF, we define an inverse quantity denoted as *time-dependent antiparallel spin electron localization function* [TDALF(x, t)] as

$$\text{TDALF}(x, t) = [1 + |P_{\alpha\beta}(x, t)/F_{\alpha}(x)|^2]^{-1}, \quad (6)$$

^{a)} Author to whom correspondence should be addressed. Fax: +49-931-888-6362. Electronic mail: voen@phys-chemie.uni-wuerzburg.de

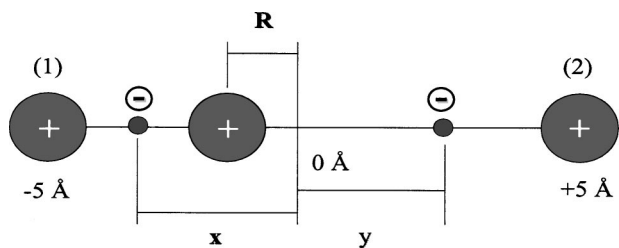


FIG. 1. Configuration of the model system: An ion (coordinate R) and two electrons (at x and y) are allowed to move between two fixed ions (1) and (2), fixed at a distance of 10 \AA .

where $F_\alpha(x)$ is the Thomas-Fermi kinetic energy density. In the case of antiparallel electron spins and within our one-dimensional model system, the latter takes the form

$$F_\alpha(x) = \frac{4}{3}\pi^2 \rho_\alpha^3(x), \quad (7)$$

where the spin density $\rho_\alpha(x)$ is normalized to 1.

The case of parallel spin is more complicated since the above defined probability $P_{\alpha\alpha}(x, x, t)$ is in fact zero due to exchange symmetry. Following Becke and Edgecombe, we first introduce the relative coordinate $s = x - y$. For our linear system, a spherical average¹ is neither necessary nor possible and the conditional probability [Eq. (4)] is directly expanded in a Taylor series up to second order around the point $s = 0$:

$$P_{\alpha\alpha}(x, s, t) = P_{\alpha\alpha}(x, 0, t) + \frac{\partial P_{\alpha\alpha}}{\partial s}(x, 0, t)s + \frac{1}{2} \frac{\partial^2 P_{\alpha\alpha}}{\partial s^2}(x, 0, t)s^2. \quad (8)$$

Since the wave function for the two-electron ($\alpha\alpha$) system has a node at $s = 0$, the constant term vanishes identically. Furthermore, according to Kato's cusp theorem,⁴ the many-body wave function Ψ is proportional to s for small s , so that $|\Psi|^2$, D , and P go like s^2 in this limit. As a consequence, the first nonvanishing term in the expansion (8) is of quadratic order and can be written as

$$P_{\alpha\alpha}(x, s, t) = \frac{1}{2} \frac{\partial^2 P_{\alpha\alpha}}{\partial s^2}(x, 0, t)s^2 = a_{\alpha\alpha}(x, t)s^2. \quad (9)$$

The function $a_{\alpha\alpha}(x, t)$ now enters directly into the definition of the time-dependent electron localization function (TDELFF) as

$$\text{TDELFF}(x, t) = [1 + |a_{\alpha\alpha}(x, t)/F_\alpha(x)|^2]^{-1}, \quad (10)$$

where $F_\alpha(x)$ is the Thomas-Fermi kinetic energy density. In the case of parallel spins $F_\alpha(x)$ is given by

$$F_\alpha(x) = \frac{16}{3}\pi^2 \rho_\alpha^3(x). \quad (11)$$

The spin density $\rho_\alpha(x)$ is again normalized to 1. Armed with the above definitions we now examine numerical examples to characterize the electron localization dynamics in a system with antiparallel and parallel spin and a fully correlated electronic and nuclear motion. Below, we also investigate the time-dependent nuclear density, defined as

$$\Gamma_{\sigma\tau}(R, t) = \int dx \int dy D_{\sigma\tau}(x, y, R, t). \quad (12)$$

The model employed in the present paper extends a previously investigated model of a single electron and an ion moving on a line within two ions (1), (2) fixed at positions $R_1 = -5 \text{ \AA}$ and $R_2 = 5 \text{ \AA}$.^{5,6} Including a second electron leads to the Hamiltonian

$$H(x, y, R) = T(x) + T(y) + T(R) + V(x, y, R), \quad (13)$$

where $T(q_i)$ is the kinetic energy operator of particle i and all coordinates refer to the origin in the middle between the two fixed ions, see Fig. 1. The potential energy is parametrized in the form:

$$V(x, y, R) = \frac{Z_1 Z}{|R_1 - R|} + \frac{Z_2 Z}{|R_2 - R|} + \frac{\text{erf}(|x - y|/R_e)}{|x - y|} - \frac{Z_1 \text{erf}(|R_1 - x|/R_f)}{|R_1 - x|} - \frac{Z_2 \text{erf}(|R_2 - x|/R_f)}{|R_2 - x|} - \frac{Z \text{erf}(|R - x|/R_c)}{|R - x|} - \frac{Z_1 \text{erf}(|R - y|/R_f)}{|R_1 - y|} - \frac{Z_2 \text{erf}(|R_2 - y|/R_f)}{|R_2 - y|} - \frac{Z \text{erf}(|R - y|/R_c)}{|R - y|}. \quad (14)$$

The first three terms describe the interaction of the nuclei with charges Z_n , Z and the electron-electron interaction. In the latter, as well as in the electron-nuclei interactions [additional terms in Eq. (14)], a screened interaction is used. Its parametrization employs error functions (erf) and screening parameters R_f (fixed ion electron), R_c (moving ion electron), and R_e (electron electron). The choice of these parameters allows one to switch between cases of weak and strong nonadiabatic interactions.⁵⁻⁹

A simpler form of this model system, containing only a single electron was used earlier by Shin and Metiu to describe charge transfer processes in crystals^{5,6} and also by us to investigate the quantum dynamics of a coupled electron and nuclear motion in the presence of strong nonadiabatic coupling^{7,9} and additional interactions with external fields.⁸ The simplicity of the model systems allows for an exact treatment of all degrees of freedom beyond the usual Born-Oppenheimer approach and also contains important ingredients which are essential to describe a realistic situation of many-particle interactions in molecules. This is essential for the considerations presented in what follows.

As a first numerical example we regard the case of antiparallel spin ($\alpha\beta$). The parameters entering into the potential energy function were chosen as $Z_n = Z = 1$, $R_c = R_f = 1.5 \text{ \AA}$, and $R_e = 2.5 \text{ \AA}$. Here and below the mass of the ion was fixed to the hydrogen mass. In order to make some predictions about the dynamical behavior of the system, we first determine the adiabatic potential curves $V_n^{\sigma\tau}(R)$ for the nuclear motion. The latter are obtained from the electronic Schrödinger equation

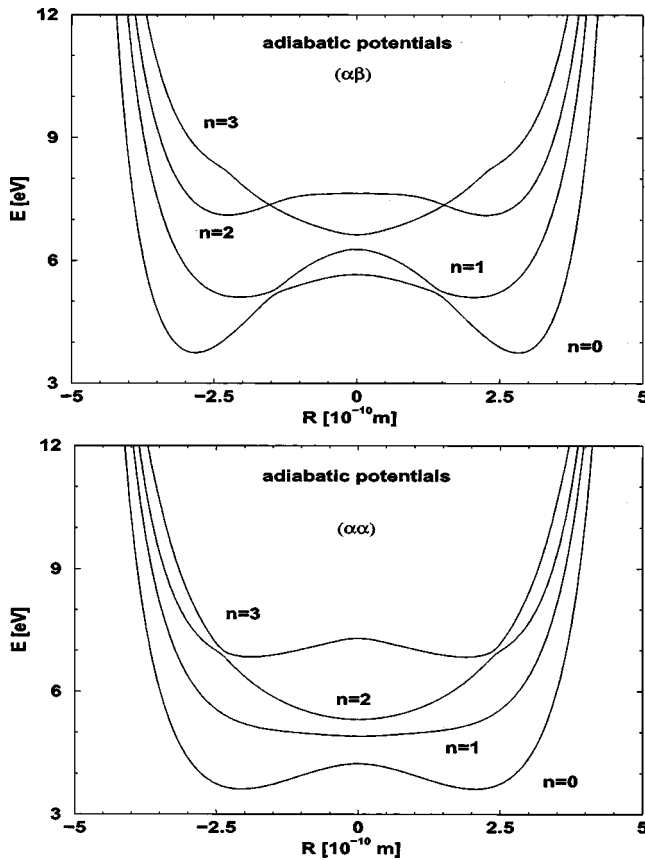


FIG. 2. Adiabatic potentials for the antiparallel (upper panel) and parallel spin case (lower panel). Different parameters were used in the parametrization of the interaction energy, as is detailed in the text.

$$\begin{aligned} & \{T(x) + T(y) + V(x, y, R)\} \phi_n^{\sigma\tau}(x, y, R) \\ & = V_n^{\sigma\tau}(R) \phi_n^{\sigma\tau}(x, y, R), \end{aligned} \quad (15)$$

so that $\phi_n^{\sigma\tau}(x, y, R)$ are the electronic eigenfunctions in state $|n\rangle$. The spin properties ($\sigma\tau$) are exclusively determined by the symmetry of the spatial wave function, so that in the (α, β) case, the eigenfunctions $\phi_n^{\sigma\tau}(x, y, R)$ are of gerade symmetry. Potential curves for the quantum numbers $n = 0-3$ are displayed in Fig. 2, upper panel. They are all bound and symmetric with respect to the origin of the coordinate system and exhibit avoided crossings at various values of R .

The time-dependent Schrödinger equation was integrated numerically using the split-operator method¹⁰ for the initial function

$$\psi(x\alpha, y\beta, R, t=0) = e^{-\gamma(R-R_0)^2} \phi_n^{\alpha\beta}(x, y, R) \quad (16)$$

with $\gamma = 0.2646 \text{ \AA}^{-2}$ and $R_0 = -3.5 \text{ \AA}$. In the present example, the initial state was localized in the first excited electronic state, i.e., we employ the electronic wave functions for $n=1$ in Eq. (16).

The nuclear density $\Gamma_{\alpha\beta}(R, t)$ (Fig. 3, upper panel) exhibits typical features of a vibrational motion where reflection at an outer turning point and the anharmonicity of the potential results in a large dispersion. A more detailed picture of the dynamics can be obtained by inspecting the populations in the various electronic states, defined as

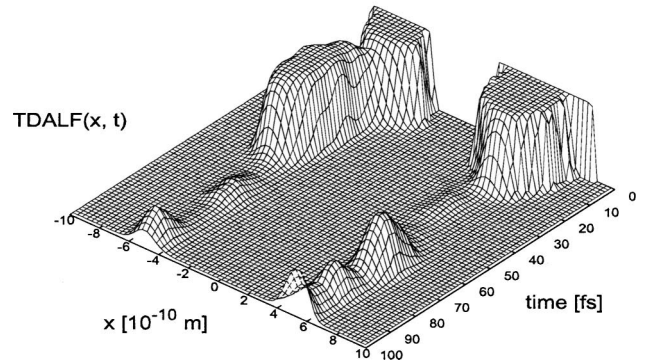
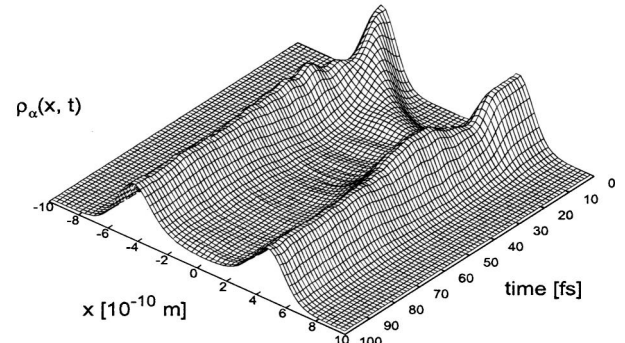
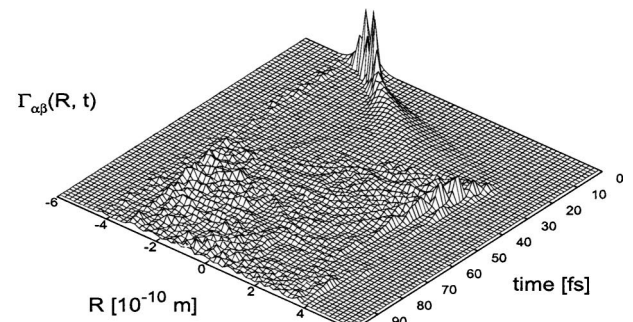


FIG. 3. Quantum dynamics in the case of anti-parallel spin. The upper panel shows the nuclear density. The time-dependent electron density and time-dependent electron localization function are shown in the middle and lower panels, respectively.

$$P_n^{\alpha\beta}(t) = \int dR |\langle \varphi_n^{\alpha\beta}(x, y, R) | \Psi(x\alpha, y\beta, R, t) \rangle_{x,y}|^2. \quad (17)$$

The populations for states $n=0, 1$ (being the only ones populated) are displayed in Fig. 4. According to the initial condition, the wave packet at early times has exclusively an excited state ($n=1$) component. After about 10 fs it reaches the first coupling region between ground and excited state at $R = -1.5 \text{ \AA}$ (see Fig. 2, upper panel). A substantial amount of population is transferred to the electronic ground state, where the motion proceeds until the moving nucleus reaches the second coupling region around $R = +1.5 \text{ \AA}$ at about 25 fs. Now the population is partially back transferred to the excited state, where the nuclear wave packet is repelled from the right fixed ion (35 fs) which gives rise to a strong oscil-

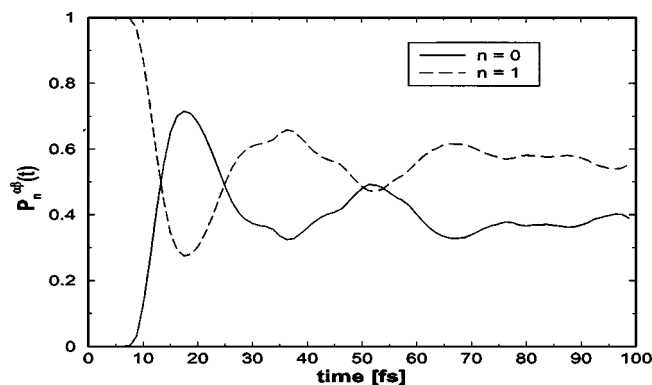


FIG. 4. Populations in the ground and first excited state for the case of antiparallel spin. Initially, only the excited state ($n=1$) is populated. Due to a strong nonadiabatic coupling, an effective population transfer between two electronic states ($n=0,1$) takes place at later times.

lation in the nuclear density. At later times the nuclear wave packet becomes extremely broad and a defined structure can no longer be seen. However, taking a look at the time-dependent electron density (Fig. 3, middle panel), it seems as if hardly anything happens. The two maxima of the electron density seen at $x = \pm 5 \text{ \AA}$ at early times, are only slightly modified by the motion of the nucleus. Thus, the electron density seems to be rather insensitive to the nuclear motion and also to the presence of nonadiabatic couplings. This can be explained by an analysis of the structure of the R -dependent electronic eigenfunctions. Although their nodal structure is different, the densities and in particular those obtained from a superposition of the two electronic states are quite similar.⁷ On the other hand, localization, if present, should be influenced more effectively. This, indeed, can be seen in Fig. 3 (lower panel) which displays the TDALF. Initially it resembles the structure of the electron density. A first effect visible in the inner localization domain (negative x values) is observed as the population transfer starts, suggesting that the electronic transition decreases the degree of localization. Within the latter time interval, however, the outer domain remains unchanged since the nucleus is still far separated from the location of ion (2). As soon as it approaches the location of the outer ion, the TDALF decreases in amplitude and nearly vanishes. Afterwards, the same effect can be seen to occur at the inner domain. Altogether, the present example illustrates that wave-packet spreading and strong nonadiabatic couplings are effective in decreasing localization. Alternatively, one can rationalize this effect taking into account that here an electronic wave packet is built and then, upon its nonstationary behavior, electron localization is diminished.

Next we treat an example where the electrons have parallel spin. Employing the parameter set $Z_n = Z = 1$, $R_c = R_e = R_f = 1.5 \text{ \AA}$, adiabatic potential curves are obtained which are shown in Fig. 2, lower panel. Here the ground state and the first excited state are well separated from each other and also from the higher states, whereas the states with $n=2$ and $n=3$ again show avoided crossings.

We solve the time-dependent Schrödinger equation numerically starting with an initial wave function as given in

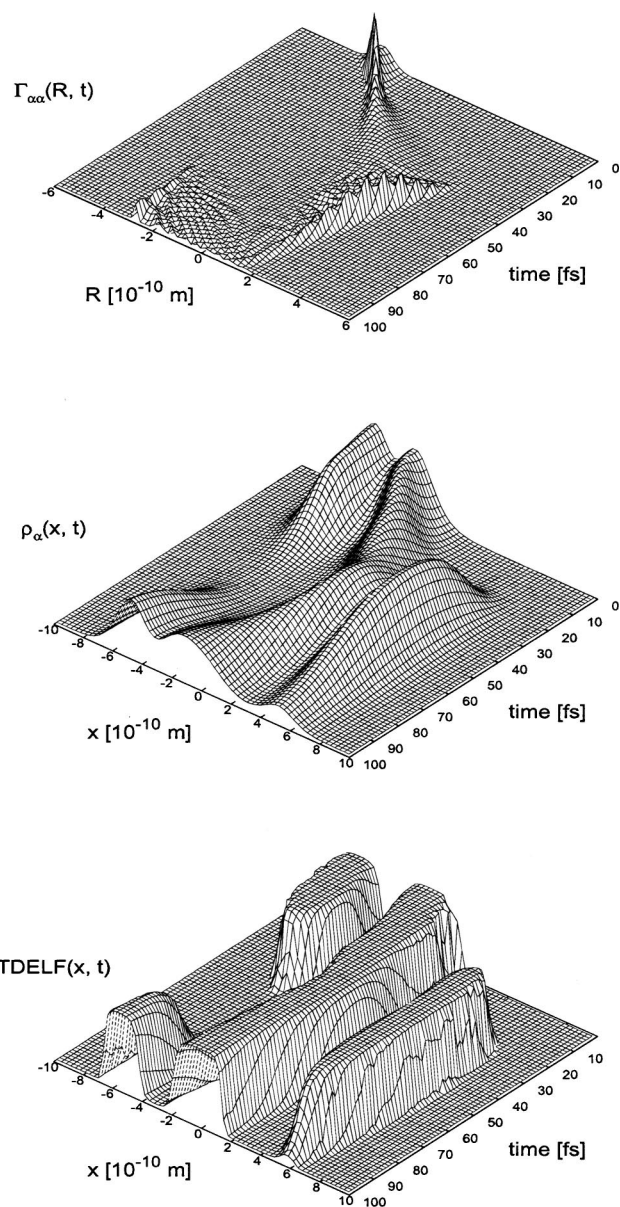


FIG. 5. Quantum dynamics in the case of parallel spin. Starting from the top, the nuclear density, the electron density, and the time-dependent electron localization function are shown in the different panels.

Eq. (16). As parameters we employed $\gamma = 0.2646 \text{ \AA}^{-2}$ and $R_0 = -2.7 \text{ \AA}$. Figure 5, upper panel, displays the calculated nuclear density $\Gamma_{\alpha\alpha}(R, t)$ (upper panel) during the vibrational motion. The particular choice of initial conditions assures that the motion takes place exclusively in a single electronic state ($n=1$). The nuclear wave packet is initially localized in the left half of the potential well and starts moving to the right side where it is repelled by the right fixed ion at about 40 fs. The incoming and outgoing (reflected) parts of the nuclear wave packet give rise to a pronounced oscillatory structure. After that, the wave packet broadens substantially due to the anharmonicity of the potential. The electron density $\rho_{\alpha}(x, t)$ (Fig. 5, middle panel) on the other hand exhibits a very smooth structure during the vibrational motion of the nucleus. At $t=0$ the electron density is accumulated around the left fixed nucleus and the moving ion and

reflects the nodal structure of the electronic eigenstate (not shown). After some time, as the nucleus crosses the origin at $R=0$, the initial density drops to zero and two new maxima occur around the right fixed nucleus and the moving ion. This can be interpreted as a charge transfer from the left fixed ion to the right one due to the motion of the nucleus. However, this situation is not fully reversed at later times because of the broadening of the nuclear probability density, so that the electron density has three maxima at about $t = 100$ fs.

From the electron density alone it is not clear how many electrons are involved in the charge transfer from the left to the right fixed ion. In order to shed some light on the process we calculated the TDELFF which is displayed in Fig. 5, lower panel. Initially it shows two localization domains: one around the left fixed ion at about $x = -5 \text{ \AA}$, the other is found near the origin ($x=0$). The first domain vanishes completely during the vibrational motion of the nucleus (it is restored at later times), while the second one is only slightly modulated. Furthermore, as the mobile ion crosses the origin of the coordinate system, a third domain, located at the right fixed ion ($x = +5 \text{ \AA}$), gets visible which drops to zero again as the vibrational period completes.

The interpretation of the TDELFF is not trivial, but the vanishing of the first domain at $x = -5 \text{ \AA}$ and the appearance of a third domain at $x = +5 \text{ \AA}$ indicates that one electron must have been removed from the left fixed nucleus and dragged to the right fixed ion as the TDELFF reveals localization of the electron distribution. Now, remembering the fact that the electron density at negative values of x drops to zero, one can conclude that both electrons participate in the charge-transfer process induced by the vibrational motion of the nucleus. During this process the maxima in the probability density of the electrons shift smoothly on the internuclear

axis. These changes are clearly reflected in the time-dependent ELF exhibiting the dynamics of the localization domains.

In conclusion, we have studied aspects of electron localization as a function of time in connection with vibrational nuclear motion. Therefore we employed exact wave functions obtained from the solution of the time-dependent Schrödinger equation for a model system. This allows for a construction of time-dependent electron localization functions in the case of parallel (TDELFF) and antiparallel (TDALFF) electron spin. The procedure is unique in the sense that the latter functions are not restricted to ground electronic states and/or approximate calculation methods and furthermore include time as well as the coupling of electronic and nuclear motion.

ACKNOWLEDGMENT

This work was funded by the Deutsche Forschungsgemeinschaft within the Graduiertenkolleg "Electron Density." Partial financial support by the EU Research and Training Network EXC!TING and by the NANOQUANTA Network of Excellence is acknowledged.

- ¹A. D. Becke and K. E. Edgecombe, *J. Chem. Phys.* **92**, 5397 (1990).
- ²A. Savin, R. Nesper, S. Wengert, and T. Fässler, *Angew. Chem., Int. Ed. Engl.* **36**, 1808 (1997).
- ³T. Burnus, M. A. L. Marques, and E. K. U. Gross, arXiv: physics/0404126v1 (27 April 2004) *Phys. Rev. A* (to be published).
- ⁴T. Kato, *Commun. Pure Appl. Math.* **10**, 151 (1957).
- ⁵S. Shin and H. Metiu, *J. Chem. Phys.* **102**, 9285 (1995).
- ⁶S. Shin and H. Metiu, *J. Phys. Chem.* **100**, 7867 (1996).
- ⁷M. Erdmann, P. Marquetand, and V. Engel, *J. Chem. Phys.* **119**, 672 (2003).
- ⁸M. Erdmann and V. Engel, *J. Chem. Phys.* **120**, 158 (2004).
- ⁹M. Erdmann, S. Baumann, S. Gräfe, and V. Engel, *Euro. Phys. J. D* (in press).
- ¹⁰M. D. Feit, J. A. Fleck, and A. Steiger, *J. Comput. Phys.* **47**, 412 (1982).